A Heterojunction Bipolar Transistor Large-Signal Model for High Power Microwave Applications [1]

Apostolos Samelis and Dimitris Pavlidis

Solid State Electronics Laboratory
Department of Electrical Engineering and Computer Science
The University of Michigan, Ann Arbor, MI 48109-2122

ABSTRACT

A large-signal model is presented for HBT's. The model accounts for self-heating effects and is based on the Gummel-Poon formulation. Full model compatibility with the commercially available software package LIBRA is ensured. The model incorporates temperature dependence for most of its parameters and has been employed for the analysis of the DC and microwave power characteristics of AlGaAs/GaAs HBT's. Good agreement between simulated and directly measured DC and microwave characteristics support the validity of the model.

I. Introduction

A major obstacle for the employment of Heterojunction Bipolar Transistors (HBT's) in high power, high frequency applications is self-heating. This is known to cause degradation of the device characteristics such as gain and can induce thermal runaway. Technological solutions that provide thermally stable HBT's have been presented recently [1], [2], [3]. Incorporation of self-heating effects in HBT large-signal models has also been reported in the past [4], [5], [6], [7]. Physically based SPICE-compatible HBT large-signal models have, finally, been presented recently [8], [9].

In this paper, the Gummel-Poon based HBT large-signal model is extended by incorporating self-heating effects and temperature dependent model parameters, such as saturation currents, current gain, junction capacitances, built-in voltages and band-gap energies. The new model is implemented in the commercially available software package HP-EESOF LIBRA. The model is, finally, validated by means of load-pull measurements.

II. Temperature Dependent Large-Signal Model

The AlGaAs/GaAs HBT used in this work was a power cell with 5 fingers and a total emitter area of $300\,\mu m^2$. Similar to [6], the model described here is complete, i.e. includes temperature dependence for most parameters. Moreover, it is based on the SPICE2 model formulation [10] which served as the basis of the large-signal analysis presented here.

The model was implemented as an user-defined SENIOR MODULE in the commercially available microwave circuit simulator, LIBRA and is shown in figure 1. Its features include high injection effects, a bias-dependent forward transit time and current crowding effects. A full temperature dependence for most of the model parameters like the zero-bias junction capacitances, the band gap, the built-in voltages, the device forward and reverse gains and the saturation currents was considered using standard SPICE proce-

TH 3B

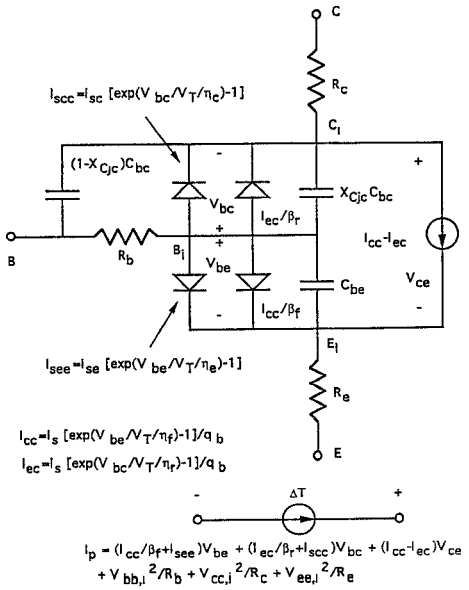

Figure 1: Temperature dependent HBT large-signal model

[1]This work has been supported by ARO (Contract No. DAAL 03-92-G-0109) and ARPA-COST (MDA 972-94-1-0004)

dures. All model equations of the SPICE2 BJT model [10] were rigorously reproduced, except the excess phase and the flicker noise parameters. A thermal sub-circuit was included and was coupled to the device so that HBT DC characteristics could be modified in the presence of thermal effects. The complete gain-temperature expression was employed as shown below:

$$\beta_f(T_2) = \beta_f(T_1)\left(\frac{T_2}{T_1}\right)^{X_{T\beta}} exp\left[\frac{q\Delta E}{k}\left(\frac{1}{T_2}-\frac{1}{T_1}\right)\right], \quad (1)$$

where T_1 and T_2 are the substrate and device temperatures respectively. Their difference, $\Delta T = T_2 - T_1$ results in a voltage difference across the thermal resistance, R_{th}, as explained below. ΔE is a constant representing the band gap difference between the emitter and base layers. As it turned out, only one parameter, namely ΔE, was sufficient for the analysis of thermal effects of the HBT under study. Therefore, the parameter $X_{T\beta}$ was assumed to be zero for the modeling purposes of this work.

The key point in the developed technique is the addition of two pins to the transistor, which permit connection of a

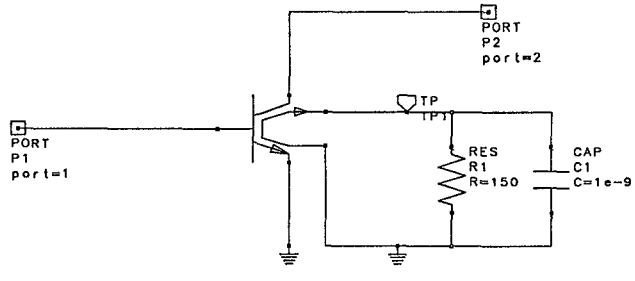

Figure 2: HBT macromodel for power HBT

current source to the HBT model in order to account for self-heating effects. The value of this current source, I_p, is equal to the power dissipated by the device and is given by,

$$I_p = (\tfrac{I_{CC}}{\beta_f} + I_{see})V_{be} + (\tfrac{I_{EC}}{\beta_r} + I_{scc})V_{bc} +$$

$$+ (I_{CC} - I_{EC})V_{ce} + \frac{V_{BB_i}^2}{R_B} + \frac{V_{EE_i}^2}{R_E} + \frac{V_{CC_i}^2}{R_C}. \quad (2)$$

This current source excites the externally connected thermal sub-circuit which consists of a thermal resistance, R_{th}, in parallel to a thermal capacitance, C_{th}. Figure 2 shows the macromodel used in the analysis of the power HBT; The thermal sub-circuit consists of $R_1 = R_{th}$ and $C_1 = C_{th}$. The HBT DC characteristics can consequently be modified when thermal effects are present by calculating the DC dissipated power, evaluating the corresponding I_p value and then coupling I_p to the HBT model through the thermal sub-circuit. Moreover, the same circuit topology can be applied to individual HBT fingers. One can in this way account for the temperature rise due to heating by adjajent fingers and evaluate therefore the overall thermal characteristics of multifinger HBT's. This approach allows an extension of the standard HBT model available in LIBRA.

All node currents, charges and their derivatives were defined in LIBRA. The latter not only involved voltage- but also temperature-dependent quantities. The linearized (small-signal) device model was developed, including temperature dependent small-signal current sources parallel to the base-emitter and base-collector conductances. Finally, the derivatives $\frac{dI_p}{dV_{be}}$, $\frac{dI_p}{dV_{bc}}$ and $\frac{dI_p}{dT}$ of the current source, I_p, of the thermal subcircuit were analytically calculated and added to the model. The inclusion of these derivatives in the model allowed better convergence of the harmonic balance algorithm.

III. Device Characterization and Model Parameter Estimation

The device model parameters were empirically extracted from DC data. The forward collector current parameters I_S and η_f were estimated by fitting of the forward Gummel-plot. The saturation current, I_{SE}, and ideality factor, η_e of the base-emitter recombination diode were empirically specified from the measured I_B data. Similarly, the reverse operation related parameters, I_{SR}, η_r, I_{SC} and η_c were determined from the reverse Gummel-plots.

The ideal forward common emitter gain, β_f, was adjusted to obtain a good fit of the $I_C - V_{CE}$ characteristics of the device in the low current active region where thermal effects are usually not significant. Finally, the reverse common-collector current gain, β_r, was set to a value of 0.1 so that the I_E/β_r-base current component could be kept small. The latter was necessary since, the emitter current was smaller than the total base current by more than two orders of magnitude.

Assuming that in the reverse operation mode the voltage drop across R_C due to I_E is much less significant than the voltage drop across R_B and R_C due to I_B, one can easily estimate the sum of the base and collector resistances from the reverse Gummel-plots. This sum was estimated to be $R_C + R_B = 3.77\,\Omega$ and the individual R_C, R_B values were assumed to be equal to 2 and 1.77 Ω respectively. The emitter resistance was adjusted in order to obtain a good agreement in the $I_C - V_{CE}$ characteristics between the measurements and the simulation in the saturation region of operation. A value of $R_E = 4.5\,\Omega$ was found appropriate for this purpose.

R_{th} and ΔE were chosen to be 150 K/W and 0.12 eV respectively so that a proper negative slope could be obtained for the $I_C - V_{CE}$ characteristics. Values of the same order of magnitude were obtained from temperature dependent char-

acterization of other AlGaAs/GaAs HBT's. Finally, a thermal capacitance of $C_{th} = 10^{-9}$ sW/K was assumed in device modeling giving a thermal time constant of $0.15\,\mu s$ i.e. significantly larger than the period of the applied RF-signal.

Table 1 shows all parameters used for the HBT macromodel in LIBRA. Figure 3 shows the fitted and measured $I_C - V_{CE}$ characteristics of the tested device. The key DC model parameters are also included in these figures. The results demonstrate an excellent agreement between experimental and simulated characteristics.

Parameter	Value	Parameter	Value
I_S	$3.015 \cdot 10^{-21}$ A	β_f	49
β_r	0.1	η_f	1.3122
η_r	1.0535	I_{SE}	$1.238 \cdot 10^{-18}$ A
I_{SC}	$3.279 \cdot 10^{-13}$	I_{KF}	0.0
I_{KR}	0.0	η_e	1.734
η_c	1.96	V_{AF}	0.0
V_{AR}	0.0	R_C	1.7768 Ω
R_E	4.5386 Ω	R_B	2 Ω
R_{BM}	2 Ω	I_{RB}	0.0
τ_f	4 ps	τ_r	1 ps
X_{TF}	0.0	C_{JE}	50 fF
V_{TF}	1.0	I_{TF}	0.0
V_{JE}	1.4 V	M_{JE}	0.5
C_{JC}	350 fF	X_{CJC}	1
V_{JC}	1.4 V	M_{JC}	0.5
FC	0.5	$X_{T\beta}$	0.0
X_{TI}	0	α	0.0007
E_G	1.43 eV	T	300 K
β	1108	ΔE	0.12 eV

Table 1: Gummel-Poon large-signal model parameters

IV. Large-Signal Characterization and Modeling

The power characteristics of the device were measured using electromechanical tuners by FOCUS MICROWAVE Inc. The bias operating conditions were set at $I_C = 10\,mA$ and $V_{CE} = 6\,V$ and the excitation frequencies were 8 GHz (one-tone excitation) and 8 GHz and 8.0001 GHz (two-tone excitation). The nonlinear products were measured using a TEKTRONIX 2755P spectrum analyzer. Measurements taken under 50 Ω loading conditions were used in the analysis that follows.

The capacitive components of the HBT model were calculated using "cold" S-parameter measurements, i.e. measurements under $I_B = 0$ and variable V_{CE} conditions as previously described by the authors [11]. The parasitic pad capacitances at the input and output of the device were extracted from these measurements and were both determined to be $C_{p1} = C_{p2} = 166\,fF$. The base-collector capacitance, C_{BC} was analytically calculated from bias dependent S-parameter data [12]. Its zero-bias value was found to be $C_{jc} = 350\,fF$. Furthermore, the forward transit time was chosen as $\tau_f = 4\,ps$ and the zero-bias emitter junction capacitance was chosen as $C_{je} = 50\,fF$. Both τ_f and C_{je}, however, were not found to affect significantly the results of the simulation.

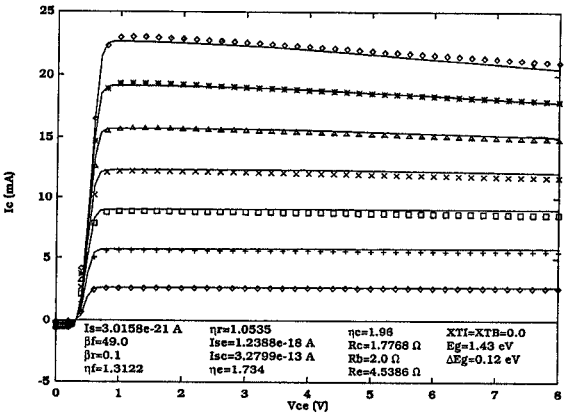

Figure 3: Measured and simulated I_C-V_{CE} characteristics of power HBT. Bottom curve: $I_B = 0.1\,mA$; Top curve: $I_B = 0.7\,mA$; I_B-step= $0.1\,mA$.

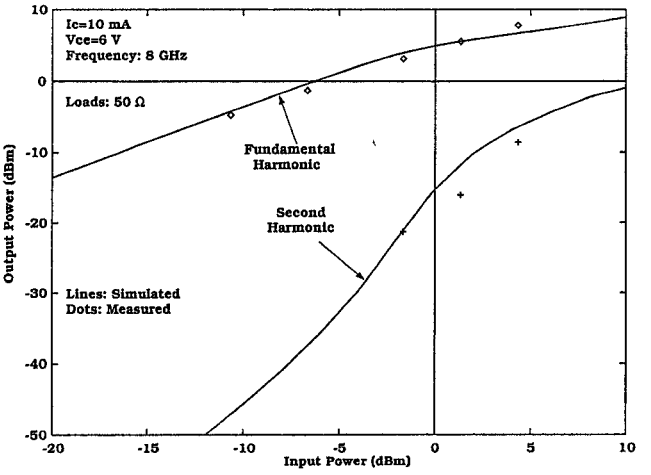

Figure 4: Power characteristics of HBT operating under one-tone excitation

The microwave power characteristics of the HBT were analyzed under single and double tone excitation using the large-signal model presented above in conjunction with LIBRA's harmonic balance simulator. Five harmonics were used to assist convergence of the algorithm.

Figure 4 shows the power of the fundamental and second harmonics generated by the device under one-tone excitation as a function of the available input power of the RF excitation, P_{in}. Figure 5 shows the power of the fundamental and

the third order intermodulation (IMD3) components generated under two-tone excitation conditions. Good agreement between the measured and simulated data is shown by the results of both figures and support the validity of the model.

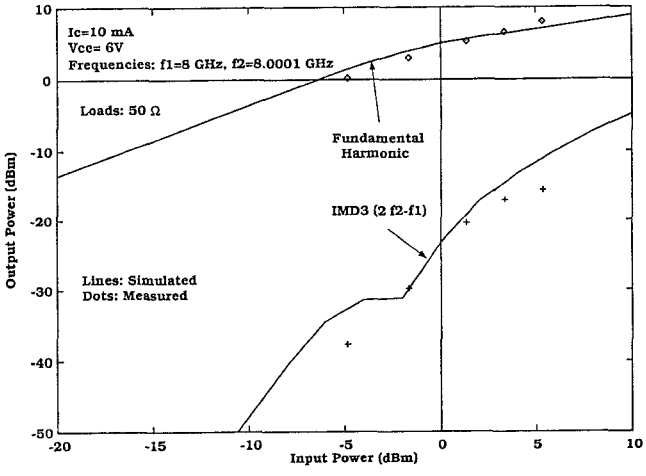

Figure 5: Power characteristics of HBT operating under two-tone excitation

V. Conclusions

A Gummel-Poon large-signal model incorporating self-heating effects was employed for the analysis of the microwave power characteristics of HBT's. The model has been incorporated in the commercially available software package LIBRA. The large-signal characteristics of AlGaAs/GaAs HBT's were analyzed by employing this model in a harmonic balance simulator. Good agreement between measurements and simulations is shown for the DC and power characteristics and suggests the suitability of the model for power analysis of HBT's. Model compatibility with LIBRA allows employment of the model in power HBT circuit simulations which account for thermal effects.

References

[1] B. Bayraktaroglou, R. Fitch, J. Barrette, R. Scherer, L. Kehias and C.I. Huang, "Design and Fabrication of Thermally-Stable AlGaAs/GaAs Microwave Power HBT's", IEEE Cornell Conference 1993 Proc., pp. 83-92.

[2] B. Bayraktaroglou, J. Barrette, L. Kehias, C.I. Huang, R. Fitch, R. Neidhard and R. Scherer, "Very High-Power-Density CW Operation of GaAs/AlGaAs Microwave Heterojunction Bipolar Transistors", IEEE Electron Device Letters, Vol. 14, No. 10, October 1993, pp. 493-495.

[3] L.L. Liou, B. Bayraktaroglou, C.I. Huang and J. Barrette, "The Effect of Thermal Shunt on the Current Instability of Multiple-Emitter-Finger Heterojunction Bipolar Transistors", IEEE 1993 Bipolar Circuits and Technology Meeting 15-3, pp. 253-256.

[4] P. Baureis, D. Seitzer and U. Schaper, "Modeling of Self-Heating in GaAs/AlGaAs HBT's for Accurate Circuit and Device analysis", 1991 GaAs-IC Symposium Digest, pp. 125-128.

[5] D.S. Whitefield, C.J. Wei and J.C.M. Hwang, "Temperature-Dependent Large Signal Model of Heterojunction Bipolar Transistors", GaAs IC Symposium 1992, pp. 221-224.

[6] C. McAndrew, "A Complete and Consistent Electrical/Thermal HBT Model", IEEE 1992 Bipolar Circuits and Technology Meeting, Proceedings pp. 10.1.1-10.1.4.

[7] K. Lu, P. Perry and T.J. Brazil, "A New SPICE-Type Heterojunction Bipolar Transistor Model for DC, Microwave Small-Signal and Large-Signal Circuit Simulation", MTT-S 1994, pp. 1579-1582.

[8] Q.M. Zhang, J. Hu, J. Sitch, R.K. Surridge and J.M. Xu, "A New Large-Signal HBT Model", MTT-S 1994 Digest, pp. 1253-1256.

[9] V. Krozer, M. Ruppert, W.Y. Lee, J. Grajal, A. Goldhorn, M. Schussler, K. Fricke and H.L. Hartnagel, "A Physics-Based Temperature-Dependent SPICE Model for the Simulation of High Temperature Microwave Performance of HBT's and Experimental Results", MTT-S 1994 Digest, pp. 1261-1264.

[10] G. Massobrio and P. Antognetti, "Semiconductor Device Modeling with SPICE", McGraw Hill, 2nd Edition, 1993, pp. 45-130.

[11] A. Samelis, D.R. Pehlke and D. Pavlidis, "Volterra Series Based Nonlinear Simulation of HBT's Using Analytically Extracted Models", Electronics Letters, 23rd June 1994, Vol. 30, No.13, pp. 1098-1100.

[12] D.R. Pehlke and D. Pavlidis, "Evaluation of the Factors Determining HBT High-Frequency Performance by Direct Analysis of S-Parameter Data", IEEE Transactions on MTT, Vol. 40, No. 12, December 1992, pp. 2367-2373.